On Enhancing Resilience to Cascading Failures via Post-Disturbance Tweaking of Line Reactances

Ali Faghih and Munther A. Dahleh, *Fellow, IEEE*

***Abstract*—The primary goal of this paper is to develop an optimization framework for studying the efficacy of transmission line reactance tweaking as a mechanism for post-disturbance control in a transmission network. We start by developing a mixed-integer linear programming (MILP) formulation for tracking the redistribution of direct current (DC) flows and the graph-theoretic evolution of a network topology over the course of cascading failures. Next, we propose a min–max setup for studying the impact of post-disturbance reactance tweaking on the resilience of the system to a worst-case disturbance. We devise a MILP reformulation scheme for the underlying bilevel non-convex mixed-integer nonlinear program to facilitate the computation of its globally optimal solution. We then develop a MILP framework for computing a tight upper bound (best-case scenario) on the efficacy of post-disturbance reactance tweaking for a given set of bus loads. Our numerical case study suggests that post-disturbance reactance tweaking, even on only a small number of lines, can be effective in reducing the amount of load shed in some scenarios in the tested system.**

***Index Terms*—Cascading failures, flexible AC transmission systems (FACTS), post-contingency control, mixed-integer bilevel programming, global optimization.**

I. Introduction

OVER the past two decades, large-scale cascading failures in various power systems have highlighted the need for substantially more effective mechanisms to increase power systems' resilience to disturbances. As a result, identifying various strategies and technologies that can increase the resilience of a power system to cascading failures has been a core topic of interest in the power systems literature. Particularly, many resilience enhancement strategies have focused on post-disturbance control. Their objective has often been to maximize the amount of demand that can be satisfied after a disturbance while returning the system to reliable operating conditions. To that end, much attention has been given to the transmission system due to its significant impact on the propagation and control of cascading failures. Transmission line switching, intentional islanding, and controlled load-shedding have been studied extensively in the existing literature (e.g. see [1]–[3] and the references therein). The existing research suggests that these well-studied mechanisms can be quite effective. However, as the demand for electricity grows and uncertainty in the system increases, there seems to be a need for technologies that can allow the system to remain resilient even at higher loading levels and in the face of a broader array of contingencies.

In this paper, we study "reactance tweaking" as a mechanism for post-disturbance control in a transmission network. The core idea behind this mechanism is simple: after the redistribution of power flows due to line failure, some lines become overloaded while some other lines have some residual capacity remaining; optimal tweaking of line reactances could reduce the flow in overloaded lines and direct it to those lines that have some unused capacity. Using the direct current (DC) approximation to alternating current (AC) power flows, we develop a framework for assessing the efficacy of this mechanism. In particular, we first develop a MILP model for tracking the evolution of network topology and redistribution of DC flows as cascading failures propagate over multiple stages. We then study the efficacy of post-disturbance reactance tweaking in response to a disturbance that seeks to cause the worst-case-scenario load-shedding by removing k lines from the network. Next, we develop a framework for computing an exact upper bound (best-case scenario) on the efficacy of post-disturbance reactance tweaking in response to any $N-k$ contingency for a given k and a given load level (an "$N-k$ contingency" is a disturbance that is initiated by the failure of up to k out of N lines). We conclude by presenting a set of numerical experiments to study the worst- and best-case efficacy of this mechanism on a test system.

This research is in line with the recent surge in both academic research and industrial interest regarding incorporation of power electronic technologies into the transmission grid for more sustainable, reliable, and flexible operation of the system. One set of technologies and devices that can provide flexibility in the system are the Flexible Alternating Current Transmission Systems (FACTS) (see e.g. [4] and [5]). The FACTS device most relevant to the study in this paper is the Thyristor-Controlled Series Compensator (TCSC). According to [4], TCSC provides

Manuscript received December 1, 2018; revised April 8, 2019 and May 26, 2019; accepted June 1, 2019. Date of publication June 12, 2019; date of current version October 24, 2019. This work was supported by the National Science Foundation Award ECCS-1135834. Paper no. TPWRS-01754-2018. *(Corresponding author: Ali Faghih.)*

A. Faghih was with the Department of Electrical Engineering and Computer Science and the Laboratory for Information and Decision Systems, Massachusetts Institute of Technology, Cambridge, MA 02139 USA (e-mail: faghih.a@gmail.com).

M. A. Dahleh is with the Department of Electrical Engineering and Computer Science and the Institute for Data, Systems, and Society, Massachusetts Institute of Technology, Cambridge, MA 02139 USA (e-mail: dahleh@mit.edu).

This paper has supplementary downloadable material available at http://ieeexplore.ieee.org, provided by the authors.
Color versions of one or more of the figures in this paper are available online at http://ieeexplore.ieee.org.
Digital Object Identifier 10.1109/TPWRS.2019.2922288

flexible (and smooth) control of the impedance of a transmission line with considerably quicker response relative to traditional control technologies, and the utilization of this device in various applications such as enhancement of transient stability, preventing voltage collapse, and improving system reliability has been studied in the literature (e.g. see [6]–[8]). The application of TCSC that is most relevant to the work in this paper is its use for mitigating transmission line overloads and reducing congestion/losses. This application of TCSC appears to have received less attention in the literature than the above-mentioned applications, though multiple papers such as [4] and [9]–[11] have studied the value of TCSC in reducing line overloads from various aspects, mostly for the case of an $N-1$ contingency and particularly for the application of security-constrained economic dispatch, suggesting that TCSC can enhance the system's security. However, none of these works have evaluated reactance tweaking from the same perspective as the model presented herein. The optimizations presented in this paper are mainly for offline assessment of worst-case load loss and best-case efficacy scenarios of adjusting TCSC post-disturbance, and therefore, are generally meant to be performed for contingency analysis at the time of power system planning. Although our results can be extended to be applied in online congestion management, this direction is not considered in this paper.

From a high-level perspective, this paper is also related to numerous works that have focused on identifying a small group of lines whose failure results in a power system that can no longer satisfy a prescribed minimum amount of demand (see e.g. [12]–[15]). To simplify numerical computations, many such studies have used DC flow equations as an approximation. Many of the models proposed for resilience assessment of power systems are in the form of bilevel (e.g. min-max) and trilevel (e.g. min-max-min) optimization problems (see, e.g. [1], [13], [16], and [17]) in which an adversarial agent and a system operator (SO) optimize their decisions strategically. Resilience is then typically measured by the load lost due to a worst-case disturbance despite the SO's post-disturbance control. Such problems are often referred to as "network interdiction" problems. The literature on bilevel network interdiction problems with purely linear and continuous inner-level programs is extensive. When the inner-level problem is bounded and feasible, a common technique is to reformulate the bilevel program into a one-level MILP by invoking the strong duality of the inner-level linear program (LP) and linearizing the integer$\times$continuous bilinear terms (e.g. see [18]). On the other hand, the literature on network interdiction problems with mixed-integer inner-level optimization problems (such as the problem of interest in this paper) is more recent and not as extensive. In terms of optimization theory, generally speaking, both analytical characterization and computational complexity of problems with mixed-integer inner-level programs are considerably more challenging. This is because strong duality no longer holds and the integer inner-level variables add non-convexity to the problem. A majority of the previous work on interdiction problems with mixed-integer inner-level optimization has dealt with "transmission line switching"; some examples of works in this line of literature include [1], [3], and [19] in which different techniques varying from locally optimal heuristics (such as the genetic algorithm and multi-start Benders decomposition methods) to global optimization techniques have been employed. The column-and-constraint generation framework presented in [1] shall be used extensively in this paper as well. However, none of these works have studied reactance tweaking in their formulation, and their underlying optimization problems are different from ours.

More recently, [20] and [21] have studied the problem of reactance tweaking under two separate models. Both models are different from ours and cover other disturbance scenarios than what is studied herein. Moreover, neither study involves mixed-integer programming, which makes their mathematical contributions also different from ours. In particular, [20] focuses on disturbances caused by changes in line impedances using AC power flow equations; however, in their post-disturbance system restoration model, line impedance is not a decision variable of interest, which makes their underlying optimization problem quite different from ours. The model studied in [21] focuses on disturbances caused by balanced changes in the supply-demand vector. Under that model, they study the margin of robustness in DC flow networks where link susceptances can be tweaked in response to a disturbance. Because of the difference in the nature of the disturbances studied, their optimization model and contributions are different from ours.

A. Summary of Contributions

The contributions of this paper can be summarized as follows:

1) We develop a MILP model for tracking the evolution of network topology and redistribution of DC flows as cascading failures propagate over multiple stages.
2) We build a bilevel optimization framework for worst-case efficacy assessment of post-disturbance reactance tweaking in response to $N-k$ contingencies. We give a rigorous framework for deriving a MILP reformulation of the underlying non-convex bilevel mixed-integer nonlinear program (MINLP), which involves nonlinearities stemming from both binary$\times$continuous and continuous$\times$continuous bilinear terms in the inner-level problem. The continuous$\times$continuous bilinear terms pose a significant computational burden for computing the globally optimal solution. However, we manage to develop exact reformulation techniques to solve this problem as a MILP by shifting the nonlinearity from the continuous$\times$continuous bilinear terms to auxiliary binary variables that are introduced into the problem as linear terms. This allows us to then tailor existing MILP-based decomposition techniques (see e.g. [1]) to our MILP reformulation and solve the underlying bilevel non-convex MINLP to global optimality. Considering that a large number of variables and constraints could exist in the underlying MINLP for a real-world large-scale power system, it is noteworthy that our MILP reformulation allows for use of existing powerful MILP methods which are "mature" in the sense that they are fast, robust, and capable of handling large problems with millions of variables (see [22]).
3) We develop a single-level MILP framework for calculating a performance upper bound (best-case efficacy) for post-disturbance reactance tweaking in response to the set of all $N-k$ contingencies.

4) The optimization framework we shall develop here can be used by researchers to study other relevant models of post-disturbance control in future research. For instance, because our model can handle integer variables at the inner level, it can be applied for combining reactance tweaking with some other means of post-disturbance control that are discrete in nature (e.g. combining reactance-tweaking with line-switching).

II. Notation and Nomenclature

Mathematical Notation:

- $|\cdot|$ For a finite set X, its cardinality shall be denoted by $|X|$; however, for a vector or matrix X, $|X|$ shall denote the absolute value of X
- The vector corresponding to any particular parameter is represented in bold-face, and the i-th entry of a vector $\mathbf{x}$ is denoted by x_i
- $\{\mathbf{x}\}$ With a slight abuse of notation, for a vector $\mathbf{x}$, we denote by $\{\mathbf{x}\}$ the set of all entries of $\mathbf{x}$
- $\text{diag}(\mathbf{x})$ A diagonal matrix whose diagonal entries are the elements of a vector $\mathbf{x}$
- For a matrix A, its transpose is denoted by A'
- $\mathbf{1}$ Denotes a vector of all ones
- $< A > \equiv < B >$ Denotes the equivalence of A and B

Network topology:

- $\mathcal{B}$ The finite set $\mathcal{B} = \{1, ..., n\}$ of buses (nodes)
- $\mathcal{E}$ The finite set $\mathcal{E} = \{1, ..., N\}$ of lines (edges)
- $(\mathcal{B}, \mathcal{E})$ This pair denotes a directed multigraph
- n The number of nodes (buses)
- N The number of lines. Each line is indexed by an integer in the set $\{1, \dots N\}$.
- $s(L)$ For a line $L = (c, d, h) \in \mathcal{E}$, extending from bus $c \in \mathcal{B}$ to bus $d \in \mathcal{B}$ and indexed by h, we define $s(L) \stackrel{\text{def}}{=} c$ (i.e. the start bus of the line)
- $e(L)$ For a line $L = (c, d, h) \in \mathcal{E}$, extending from bus $c \in \mathcal{B}$ to bus $d \in \mathcal{B}$ and indexed by h, we define $e(L) \stackrel{\text{def}}{=} d$ (i.e. the end bus of the line)
- $\mathcal{E}_i$ The set of all lines incident to node i
- M The *incidence matrix* is a $|\mathcal{B}| \times |\mathcal{E}|$ matrix in which every entry $M_{BL} = 1$ if $B = s(L)$ and $M_{BL} = -1$ if $B = e(L)$, and $M_{BL} = 0$ otherwise

Transmission line characteristics:

- $\overline{C}^a_{ijh}$ The active (operational) flow carrying capacity of line (i, j, h) (i.e. line (i, j, h) is guaranteed to be active as long as the power it carries is below $\overline{C}^a_{ijh}$)
- $\overline{C}^f_{ijh}$ The failing capacity threshold of line (i, j, h), i.e. line (i, j, h) is guaranteed to fail as soon as the power it carries reaches (or exceeds) $\overline{C}^f_{ijh}$
- $x^{\min}_{ijh}$ ($x^{\max}_{ijh}$) The minimum (maximum) allowed reactance for line (i, j, h) after tweaking
- x^o_{ijh} The reactance of line (i, j, h) before tweaking (note that $x^o_{ijh} \in [x^{\min}_{ijh}\ x^{\max}_{ijh}]$ by assumption)

Parameters for power flow and cascading failures:

- T The time-horizon of the cascade, i.e. the number of stages for which the cascading failures propagate before the system operator's response
- $\mathbf{b}^t$ The vector of net bus injections at time $t \leq T$
- $\mathcal{B}^o_{\pm}$ The set of all buses with non-zero injections at $t = 0$
- θ^t The vector of all bus phase angles at time t
- I^t_{ijh} The power flow (DC) in line (i, j, h) at time t
- z^t_{ijh} Binary variable indicating the failure state of line (i, j, h) at the end of time t ($z^t_{ijh} = 1$ if the line is active by the end of stage t, and $z^t_{ijh} = 0$ otherwise)
- s^t_{ijh} Binary variable that switches from 1 to zero at time t if line (i, j, h) trips at time t (if line (i, j, h) has already failed prior to stage t, then $s^t_{ijh} = 0$)
- y^t_i Binary variable indicating the islanding of node i at the end of time t ($y^t_i = 0$ if the node has been islanded by the end of stage t, and $y^t_i = 1$ otherwise)
- $i \overset{t}{\leftrightarrow} j$ Indicates that an active path exists between buses i and j at the end of stage t
- $i \overset{t}{\nleftrightarrow} j$ Indicates no active path exists between buses i and j at the end of stage t

Remark 1: Transmission lines are usually denoted by the pair of buses belonging to their end nodes. However, it is possible that more than one line connect a pair of buses to each other, like in the test system presented in our case study in Section VI. This is why we denote transmission lines using a triplet.

III. Modeling Cascading Failures

In this section, we shall develop a MILP model for tracking the evolution of network topology and redistribution of flows as cascading failures propagate over multiple stages. We will use the DC approximation to AC power flows (see e.g. [23]); thus: $P_{ijh} = (\theta_i - \theta_j)/x_{ijh}$, where P_{ijh} denotes the real power flow on line (i, j, h), θ_i denotes the phase angle at node i and x_{ijh} denotes the line's reactance.

Remark 2: To mitigate the computational burden of dealing with AC flow equations, we shall use the DC approximation like many other related studies in the existing literature have done (e.g. [1], [16], [18], [19], and [21]). However, it should be acknowledged that it would be more realistic to capture the full AC flow equations including both active and reactive power flow to give a more comprehensive analysis.

We shall focus our attention only on the set of disturbances that do not cause generation-load imbalances during the propagation of cascading failures. Generally speaking, imbalances between generation and load need to be resolved quickly, because otherwise, the frequency's deviation from the nominal value might jeopardize the power system's stability and security (e.g. see [24]). Dealing with generation-load imbalances in our multi-stage model would add a significant layer of computational complexity to the underlying optimization problem. Thus, we shall impose the constraint that all load and generation buses remain connected to each other for the duration of cascading failures. This will ensure that the load and generation remain equal throughout the propagation of cascading failures. Combining reactance-tweaking with problems such as dynamic load-shedding for disturbances involving generation-load imbalances is a related problem that merits its own line of future research. Nevertheless, the graph-theoretic techniques that we

develop in this paper are general and can be extended to model settings with demand-generation imbalances.

Remark 3: The DC power flow model presented here does not account for reactive power when dealing with overloaded lines and reactance tweaking; however, controlling reactive power in the presence of FACTS devices is an important related problem and we refer interested readers to e.g. [5], [25], and the references therein for detailed discussions.

A. Modeling the Evolution of the Graph Topology Prior to the System Operator's Response

In our model, the "adversary", which initiates the cascading failures, causes a disturbance at time $t = 0$ by simultaneously removing up to k lines from the grid. After that, the adversary takes no further action, and cascading failures propagate for T discrete stages. We assume that the only source of the propagation is the failure of new lines at each stage due to the redistribution of flows under the new network topology. We further assume that any line trips at time $t + 1$ if its flow capacity threshold is exceeded at time t and that line capacities remain the same before and after reactance tweaking.

Remark 4: While we only focus on cascades caused by line failures, other modes of cascades such as those induced by voltage and transient stability issues, etc. are also possible. Once we lay the groundwork for these simpler/stylized cascade scenarios, future research can build on that to address more complex modes of cascades.

The binary *tripping state* of line (i, j, h) due to the disturbance at time 0 is binary: $s^0_{ijh} = 0$ if (i, j, h) is tripped by the adversary and $s^0_{ijh} = 1$ otherwise. Next, we check if the disturbance has disconnected any nodes from $\mathcal{B}^o_{\pm}$ by defining the binary *connectedness state* of a node i at stage t, denoted by y^t_i. If $y^0_i = 1$, node i is still connected to $\mathcal{B}^o_{\pm}$ and if $y^0_i = 0$ it has been islanded at time 0. We shall set one node $g \in \mathcal{B}^o_{\pm}$ as the reference node, and determine the value of $\mathbf{y}^t$ based on whether each node is connected to g or not. The binary *failure state* of line (i, j, h) at stage 0, z^0_{ijh}, determines whether line (i, j, h) has failed (either due to tripping or due to islanding).

The nomenclature follows the same procedure for $t \geq 1$. The only distinction is that for $t \geq 1$, the binary tripping state of a line (s^t_{ijh}) will only change if line (i, j, h) trips due to overloading at stage t. This is because the adversary is no longer part of the game and the cascade is propagating purely due to the natural redistribution of flows following the initial disturbance. Note also that z^t_{ijh} takes into account both forms of line failure, and hence, it is updated at the end of stage t. Thus, $z^t_{ijh} \leq s^t_{ijh}\ \forall t$, and $s^t_{ij} \leq z^{t-1}_{ijh}$ for $t \geq 1$.

Proposition 1: In order for the failure indicator $\mathbf{z}^t$ to take a value of 0 for either a disconnected or a tripped line, but *not* take on a value of 0 for an active line, it is a necessary condition that the following hold:

$$|M'|\mathbf{y}^t \geq \mathbf{z}^t \geq \mathbf{s}^t + |M'|\mathbf{y}^t - 2,\ \mathbf{s}^t \geq \mathbf{z}^t,\ \forall t \geq 0$$

Using the following theorem, we derive a full MILP approach for tracking whether a line/node is still connected to another node at the end of each stage.

Theorem 1: Given a binary vector $\mathbf{y}^t \in \{0,1\}^{|\mathcal{B}|}$ with $y^t_g = 1$, if for some $\mathbf{e}^t \in \{0,1\}^{|\mathcal{B}|}, \mathbf{p}^t \in \{0,1\}^{|\mathcal{B}|}, \mathbf{u}^t \in \{0,1\}^{|\mathcal{E}|}, \mathbf{w}^t \in \{0,1\}^{|\mathcal{E}|}$ we have

$$\begin{aligned}
&\mathbf{s^t} + \mathbf{w^t} - y^t_i\mathbf{1} \leq \mathbf{1},\\
&-\mathbf{w^t} \leq M'\mathbf{p^t} \leq \mathbf{w^t},\\
&p^t_g = 0,\\
&p^t_i = 1 - y^t_i,\\
&\sum_{\ell \in \mathcal{E}_n} u^t_\ell = 2e^t_n\ \forall n \neq g, n \neq i\\
&\sum_{\ell \in \mathcal{E}_g} u^t_\ell = y^t_i, \sum_{\ell \in \mathcal{E}_i} u^t_\ell = y^t_i,\\
&\mathbf{u}^t \leq \mathbf{x}^t,\ \mathbf{e}^t \leq \mathbf{y}^t,\ \mathbf{e}^t \leq y^t_i\mathbf{1}
\end{aligned} \tag{1}$$

then $< g \overset{t}{\leftrightarrow} i > \equiv < y^t_i = 1 >$ and $< g \overset{t}{\nleftrightarrow} i > \equiv < y^t_i = 0 >$.

The key ideas in the above theorem are "cut removal" and "path existence". When a node i has been islanded away from another node g, it means that an $i - g$ cutset (please see E-Companion XI for definition) has been removed from the graph. Conversely, if i and g are connected, at least one path has to exist between them. The above result provides a general framework for tracking the evolution of the topology as cascading failures propagate. However, as mentioned earlier, since we are focusing on the case of disturbances that do not cause demand-generation imbalances, we shall impose for any bus $q \in \mathcal{B}^o_{\pm}$ the constraint that $y^t_q = 1$ for all $t \leq T - 1$, while leaving the y^t_j as free binary variables for all $j \notin \mathcal{B}^o_{\pm}$.

B. Modeling the Redistribution of Flows

It remains to describe how the redistribution of flows is tracked. To do this, we first compute Kirchhoff's Current Law (KCL) and Kirchhoff's Voltage Law (KVL) equations at each stage: $M\text{diag}(\mathbf{z}^{t-1})\mathbf{I}^t = \mathbf{b}^t$ (KCL) and $\text{diag}(\mathbf{x}^o)\text{diag}(\mathbf{z}^{t-1})\mathbf{I}^t = \text{diag}(\mathbf{z}^{t-1})M'\theta$ (KVL), $\forall t \geq 1$.
Next, by setting $(z^{t-1}_{ijh} + s^t_{ijh} - 1)|I^t_{ijh}| \leq \overline{C}^a_{ijh}\,\forall (i, j, h) \in \mathcal{E}, \forall t \geq 1$ we ensure that the flow in any line that has not failed by the end of stage $t - 1$ and not tripped at stage t is below its capacity limit. This inequality becomes redundant if the line has failed by the end of $t - 1$ or is tripping at t. Similarly, we enforce $z^{t-1}_{ijh}|I^t_{ijh}| \geq \overline{C}^f_{ijh}(z^{t-1}_{ijh} - s^t_{ijh})\,\forall (i, j, h) \in \mathcal{E}, \forall t \geq 1$ to ensure that any line that trips at stage t had first survived by the end of stage $t - 1$ and then overloaded at stage t. Note that the absolute value terms and binary×continuous product terms in the above equations can be linearized using standard techniques described in E-Companion IX.

Please see E-Companion XII for a diagram that summarizes the approach described in Section III.

IV. Efficacy of Post-Contingency Reactance Tweaking in Response to Worst-Case Disturbance

For evaluating the efficacy of post-disturbance reactance tweaking, we first develop a framework for measuring the *worst-case* scenario. This entails calculating the worst-case amount of load that needs to be shed to restore the network in the presence of reactance tweaking. We shall refer to this worst-case scenario as the "yield-minimizing $N-k$ contingency."

A. The System Operator's Response: Reactance-Controlled Yield Maximization

Before formally stating the optimization problem, let us first introduce some additional nomenclature:

- $T+1$ The stage at which post-disturbance control is implemented by the system operator
- b_i^d The satisfied demand post-disturbance at bus i after the system operator's response
- b_i^g The amount of post-disturbance generation at bus i after the system operator's response
- b_i^{T+1} Net nodal injection at node i as per the SO's post-disturbance dispatch. Note that for the special case of $t=T+1$ (i.e. the case of post-disturbance dispatch), we have $b_i^{T+1} \triangleq b_i^g - b_i^d$ for each node i.
- $\overline{b}_i^d$ The amount of power demanded at bus i
- $\overline{b}_i^g$ The generation capacity at bus i
- τ_{ijh} Binary variable indicating whether the reactance of a line (i,j,h) at time $T+1$ is allowed to be tweaked ($\tau_{ijh}=1$ if tweaking is allowed, and 0 otherwise)
- H The total number of lines on which reactance tweaking is allowed

Definition 1: We define the "reactance-controlled yield" as the maximum demand that the SO can satisfy post-disturbance in the presence of reactance tweaking (without violating any physical constraints):

$$
\begin{aligned}
\max_{D}\quad & \sum_{i\in\mathcal{B}} b_i^d \\
\text{s.t.}\quad & I_{ijh}^{T+1}x_{ijh}^{T+1} = s_{ijh}^T(\theta_i^{T+1}-\theta_j^{T+1}),\ \forall (i,j,h)\in\mathcal{E} \\
& b_i^g - b_i^d = \sum_{(i,j,h)\in\mathcal{E}_i} I_{ijh}^{T+1},\ \forall i\in\mathcal{B} \qquad \text{(a)} \\
& x_{ijh}^{T+1} - x_{ijh}^o - \tau_{ijh}(x_{ijh}^{\max}-x_{ijh}^o) \le 0\ \forall (i,j,h)\in\mathcal{E} \\
& x_{ijh}^o - x_{ijh}^{T+1} + \tau_{ijh}(x_{ijh}^{\min}-x_{ijh}^o) \le 0\ \forall (i,j,h)\in\mathcal{E} \\
& \sum_{(i,j,h)\in\mathcal{E}} \tau_{ijh} = H\ \forall (i,j,h)\in\mathcal{E} \qquad \text{(b)} \\
& -\overline{C}_{ijh}^a \le I_{ijh}^{T+1} \le \overline{C}_{ijh}^a,\ \forall (i,j,h)\in\mathcal{E} \\
& 0\le b_i^g \le \overline{b}_i^g,\quad \forall i\in\mathcal{B} \qquad \text{(c)} \\
& 0\le b_i^d \le \overline{b}_i^d,\quad \forall i\in\mathcal{B} \qquad \text{(d)} \\
& x_{ijh}^{T+1},\theta_i^{T+1},I_{ijh}^{T+1},b_i^g,b_i^d\in\mathbb{R},\forall i\in\mathcal{B},(i,j,h)\in\mathcal{E} \\
& \tau_{ijh}\in\{0,1\},\quad \forall (i,j,h)\in\mathcal{E}. \qquad (2)
\end{aligned}
$$

where $D \triangleq \{\mathbf{x^{T+1}}, \theta^{\mathbf{T+1}}, \mathbf{I^{T+1}}, \mathbf{b}^g, \mathbf{b}^d, \boldsymbol{\tau}\}$ is the set of decision variables, and $\mathbf{s}^T \in \{0,1\}^{|\mathcal{E}|}$ is the binary vector of line failure states that is given to the problem as an input parameter. The above reactance-controlled yield maximization problem is the SO's post-disturbance control problem for restoring the system to reliable conditions.

In the above formulation, the objective is to maximize the amount of load served. The first two constraints are KVL and KCL for DC flows, the next three constraints ensure that the reactances of at most H lines can be tweaked within a prescribed range (and all the other lines will retain their original reactances), the sixth constraint ensures no line flow capacities are violated, the seventh constraint ensures that the generation capacities of each bus are not exceeded, and the eighth constraint ensures that the served load at each bus will be between zero and the original demand.

In Theorem 2 below, we develop a reformulation scheme that turns the SO's post-disturbance control problem (2) into a MILP. As discussed in the proof of this theorem in the E-Companion, we accomplish this by shifting the nonlinearity stemming from continuous$\times$continuous bilinear terms to auxiliary binary variables that we introduce into the problem in linear terms.

Theorem 2: If Γ^* is the globally optimal value of the objective function in the optimization problem (2), then

$$
\begin{aligned}
\Gamma^* = \max_{\omega}\ & \sum_{i\in\mathcal{B}} b_i^d \\
\text{s.t.}\quad & \boldsymbol{\mu} + \Upsilon(\mathbf{s}^T-1) \le M'\boldsymbol{\theta}^{T+1} \le \boldsymbol{\mu} + \Upsilon(1-\mathbf{s}^T); \\
& -\operatorname{diag}(\mathbf{s}^T)\overline{\mathbf{C}}^a \le \boldsymbol{I}^{T+1} \le \operatorname{diag}(\mathbf{s}^T)\overline{\mathbf{C}}^a; \\
& \boldsymbol{\mu} - \operatorname{diag}(\boldsymbol{x}^o)\boldsymbol{I}^{T+1} - 2\Upsilon\boldsymbol{\tau} \le 0; \\
& -\boldsymbol{\mu} + \operatorname{diag}(\boldsymbol{x}^o)\boldsymbol{I}^{T+1} - 2\Upsilon\boldsymbol{\tau} \le 0; \\
& \operatorname{diag}(\mathbf{x}^{\min})\boldsymbol{\alpha} \le \boldsymbol{\delta} \le \operatorname{diag}(\mathbf{x}^{\max})\boldsymbol{\alpha}; \\
& \boldsymbol{\alpha} = \boldsymbol{\beta} + \boldsymbol{\varphi}; \\
& \boldsymbol{I}^{T+1} = \boldsymbol{\beta} - \boldsymbol{\varphi}; \\
& \boldsymbol{\beta} - \operatorname{diag}(\overline{\mathbf{C}}^a)\boldsymbol{\upsilon} \le 0; \\
& \boldsymbol{\varphi} - \operatorname{diag}(\overline{\mathbf{C}}^a)(\mathbf{1}-\boldsymbol{\upsilon}) \le 0; \\
& \boldsymbol{\delta} = \boldsymbol{\phi} + \boldsymbol{\Phi}; \\
& \boldsymbol{\mu} = \boldsymbol{\phi} - \boldsymbol{\Phi}; \\
& \boldsymbol{\Phi} - \Upsilon(\mathbf{1}-\boldsymbol{\psi}) \le 0; \\
& \boldsymbol{\phi} - \Upsilon\boldsymbol{\psi} \le 0; \\
& \boldsymbol{\phi} \ge 0;\ \boldsymbol{\Phi} \ge 0;\ \boldsymbol{\varphi} \ge 0;\ \boldsymbol{\beta} \ge 0; \\
& \text{Constraints (a), (b), (c), (d) from Prob (2);} \\
& \boldsymbol{\alpha},\boldsymbol{\beta},\boldsymbol{\varphi},\boldsymbol{\mu},\boldsymbol{\delta},\boldsymbol{\Phi},\boldsymbol{\phi},\boldsymbol{I}^{T+1} \in \mathbf{R}^{|\mathcal{E}|}; \\
& \boldsymbol{\tau},\boldsymbol{\psi},\boldsymbol{\upsilon} \in \{0,1\}^{|\mathcal{E}|};\ \boldsymbol{\theta}^{T+1},\boldsymbol{b}^g,\boldsymbol{b}^d \in \mathbb{R}^{|\mathcal{B}|} \qquad (3)
\end{aligned}
$$

where $\Upsilon \triangleq G\sum_{(p,q,h)\in\mathcal{E}} x_{pqh}^{\max}$ and $\omega = \{\boldsymbol{\alpha},\boldsymbol{\beta},\boldsymbol{\varphi},\boldsymbol{\mu},\boldsymbol{\delta},\boldsymbol{\Phi},\boldsymbol{\phi}, \boldsymbol{I}^{T+1},\boldsymbol{\tau},\boldsymbol{\psi},\boldsymbol{\upsilon},\boldsymbol{\theta}^{T+1},\boldsymbol{b}^g,\boldsymbol{b}^d\}$. (Note that $\boldsymbol{\alpha},\boldsymbol{\beta},\boldsymbol{\varphi},\boldsymbol{\mu},\boldsymbol{\delta},\boldsymbol{\Phi},\boldsymbol{\phi}, \boldsymbol{\psi},\boldsymbol{\upsilon}$ are all auxiliary variables).

For brevity of exposition, we switched from scalar notation in (2) to matrix notation in (3) above (for a detailed description of the constraints in (3) please see the proof of Theorem 2 in the E-Companion).

By denoting the feasible set in (3) by Ω, (3) can be written in a compact form as:

$$\max_{\boldsymbol{\omega}\in\Omega} \sum_{i\in\mathcal{B}} b_i^d. \tag{4}$$

So far, we have formulated how the SO re-dispatches the system at time $T+1$ in our model. Now that we have formulated the system operator's problem, we shall describe the adversary's problem.

B. The Adversary Minimizes the Maximum Post-Disturbance Yield: A Bilevel MINLP for the Worst-Case Scenario

Given that the reactance-controlled yield problem is a maximization problem as defined in (2), the adversary's problem is a min-max bilevel program:

$$\min_{A\in\mathcal{A}} \max_{\boldsymbol{\omega}\in\Omega} \sum_{i\in\mathcal{B}} b_i^d \tag{5}$$

where A is the vector of the adversary's decision variables, and $\mathcal{A}$ is the feasible set of the adversary's problem (which are defined explicitly in (6) below). This bilevel program, which is our measure of the worst-case-scenario resilience, can now be written as:

$$\begin{aligned}
\min_{A}\ \ & \max_{\boldsymbol{\omega}\in\Omega} \sum_{i\in\mathcal{B}} b_i^d \\
\text{s.t.}\ \ & \mathbf{1}'\mathbf{s}^o \geq |\mathcal{E}| - k \\
& M\text{diag}(\mathbf{z}^{t-1})\mathbf{I}^t = \mathbf{b}^o\, \forall t \geq 1 \\
& \text{diag}(\mathbf{x}^o)\text{diag}(\mathbf{z}^{t-1})\mathbf{I}^t = \text{diag}(\mathbf{z}^{t-1})M'\theta\, \forall t \geq 1 \\
& (z_{ijh}^{t-1} + s_{ijh}^t - 1)|I_{ijh}^t| \leq \overline{C}_{ijh}^a\, \forall (i,j,h) \in \mathcal{E}, \forall t \geq 1 \\
& z_{ijh}^{t-1}|I_{ijh}^t| \geq \overline{C}_{ijh}^f (z_{ijh}^{t-1} - s_{ijh}^t)\, \forall (i,j,h) \in \mathcal{E}, \forall t \geq 1 \\
& |M'|\mathbf{y}^t \geq \mathbf{z}^t \geq \mathbf{s}^t + |M'|\mathbf{y}^t - 2\ \forall t \geq 0 \\
& y_i^t = 1\ \forall i \in \mathcal{B}_{\pm}^o, \forall t \leq T-1\ (T \geq 1 \text{ only}) \\
& \mathbf{y}^{t-1} \geq \mathbf{y}^t,\ \forall t \leq T-1\ (T \geq 1 \text{ only}) \\
& \mathbf{s}^t \geq \mathbf{z}^t\ \forall t \geq 0 \\
& \mathbf{z}^{t-1} \geq \mathbf{s}^t\ \forall t \geq 1 \\
& i \overset{t}{\leftrightarrow} j\ \forall i,j \in \mathcal{B}_{\pm}^o, 1 \leq t \leq T-1\ (T \geq 1 \text{ only}) \\
& z_{ijh}^t,\ s_{ijh}^t,\ y_q^t \in \{0,1\},\ \forall (i,j,h) \in \mathcal{E},\ \forall q \in \mathcal{B}
\end{aligned} \tag{6}$$

where $A = \{\mathbf{s}^0, \ldots, \mathbf{s}^T, \mathbf{z}^0, \ldots, \mathbf{z}^{T-1}, \mathbf{y}^0, \ldots, \mathbf{y}^{T-1}, \mathbf{I}^1, \ldots, \mathbf{I}^T, \theta^1, \ldots, \theta^T, \mathcal{P}\}$. Here, $\mathcal{P}$ denotes the set of all variables used in keeping track of the connectivity of the buses for all $t \in \{0, \ldots, T-1\}$ (which are the auxiliary variables defined in Theorem 1). In (6), the first constraint requires that the adversary trips up to k lines at $t = 0$, the second and third constraints are for KVL and KCL at each stage, the fourth and the fifth constraints keep track of the lines that have survived and failed, respectively, and the remainder of the constraints keep track of the connectivity and evolution of the topology as established in Proposition 1 and Theorem 1.

The next step is to linearize all the binary×continuous product terms and absolute value terms in problem (6) so that we can write the outer-level problem as a MILP. Doing so is a standard trick used frequently in the optimization literature, which we have summarized in E-Companion IX. For the remainder of this paper, we shall denote the set of the decision variables in the linearized reformulation of the adversary's problem by a and the feasible set of this linearized reformulation by $\tilde{a}$. The bilevel MILP reformulation of the min-max problem can then be written as

$$\min_{a\in\tilde{a}} \max_{\boldsymbol{\omega}\in\Omega} \sum_{i\in\mathcal{B}} b_i^d. \tag{7}$$

C. Solving the Bilevel MINLP Underlying the Min-Max Problem

Now that Problem (2) has been reformulated as a MILP, the min-max problem (6) can be solved to global optimality using a decomposition method involving column and constraint generation ([1], [26], [27]).

We can now formally establish how a column-and-constraint-generation scheme can be applied to our problem to obtain the globally optimal solution to problem (6). This entails deriving bounds on the dual variables in the innermost-level program in our problem. First, we turn Problem (6) into a large-scale single-level MILP. To do so, we start by separating the continuous variables in (3) from the integer ones. Let us denote the vector of integer decision variables in (3) by $\boldsymbol{\xi}$, denote the set of all $\boldsymbol{\xi}$ that maintain the feasibility of Problem (3) by $\mathcal{I}$, denote the vector of continuous decision variables in (3) by $\boldsymbol{\vartheta}$, and denote the set of the constraints in (3) that involve continuous variables (for a given $\boldsymbol{\xi}$) by $\mathcal{C}(\boldsymbol{\xi})$; then we can write Problem (3) as:

$$\max_{\boldsymbol{\xi}\in\mathcal{I}} \max_{\boldsymbol{\vartheta}\in\mathcal{C}(\boldsymbol{\xi})} \sum_{i\in\mathcal{B}} b_i^d \tag{8}$$

and since the inner-level problem above is a linear program, we can write it in standard form:

$$\max_{\boldsymbol{\vartheta}\in\mathcal{C}(\boldsymbol{\xi})} \sum_{i\in\mathcal{B}} b_i^d \equiv \max_{C\boldsymbol{\vartheta}\leq\mathbf{c}_{\boldsymbol{\xi}}} \boldsymbol{f}'\boldsymbol{\vartheta} \tag{9}$$

where $\boldsymbol{f}'\boldsymbol{\vartheta} = \sum_{i\in\mathcal{B}} b_i^d$. Then we invoke strong duality as shown in the proposition below.

Proposition 2: Strong duality holds for the inner-level problem in (8), and hence,

$$\max_{\boldsymbol{\xi}\in\mathcal{I}} \max_{\boldsymbol{\vartheta}\in\mathcal{C}(\boldsymbol{\xi})} \sum_{i\in\mathcal{B}} b_i^d = \max_{\boldsymbol{\xi}\in\mathcal{I}} \min_{C'\boldsymbol{\lambda}_{\boldsymbol{\xi}}=\boldsymbol{f}, \boldsymbol{\lambda}_{\boldsymbol{\xi}}\geq 0} \mathbf{c}'_{\boldsymbol{\xi}}\boldsymbol{\lambda}_{\boldsymbol{\xi}}. \tag{10}$$

Definition 2: We define the set of all "bilinear terms" $P(g)$ of a multivariate polynomial $g(\cdot)$ as the set of all terms in $g(\cdot)$ in which strictly two variables have degree 1 and all other variables have degree 0. The set of all "bilinear forms" $R(g)$ of a multivariate polynomial $g(\cdot)$ is then obtained by dividing each element of $P(g)$ by its scalar coefficient (please see Example 1 in E-Companion X).

Definition 3: Consider two vectors $\mathbf{p} = [p_1, p_2, \ldots, p_m]'$ and $\mathbf{q} = [q_1, q_2, \ldots, q_d]'$ for some (finite) $m, d \in \mathbb{Z}_+$. Then,

we define $\mathcal{G}(g,\mathbf{p},\mathbf{q}) \triangleq R(\mathcal{V}(\mathbf{p},\mathbf{q})) \cap R(g(\mathbf{p},\mathbf{q}))$, where $\mathcal{V}(\mathbf{p},\mathbf{q}) = \mathbf{1}'\mathbf{p}\mathbf{q}'\mathbf{1}$ and $g(\cdot)$ is a multivariate polynomial (recall that $R(\cdot)$ is the set of bilinear forms). Also, denote by F a bijective map from $\mathcal{G}(g,\mathbf{p},\mathbf{q})$ to a set $\mathbf{J}$. Then, we shall define the *substitution function* $\mathcal{J}(g,\mathbf{p},\mathbf{q},\mathbf{J},F)$ as a function that replaces in $g(\cdot)$ every instance of each element of $\mathcal{G}(g,\mathbf{p},\mathbf{q})$ with its corresponding element from $\mathbf{J}$ (as per map F); note that all the other terms in $g(\cdot)$ remain unchanged. Also, $Y_{F,\mathbf{p}} : \mathbf{J} \to \{\mathbf{p}\}$ is a surjective map that maps each element of $\mathbf{J}$ to its corresponding entry in $\mathbf{p}$ as per the change of variables defined by map F (please see Example 2 in E-Companion X).

Next, by deriving a bound on the dual variables (i.e. $\boldsymbol{\lambda_\xi}$) and enumerating over all elements of $\mathcal{I}$, we reformulate Problem (6) as a large-scale MILP as shown below.

Theorem 3: If Λ^* is the globally optimal value of the objective function in the optimization problem (6), then

$$\begin{aligned}
\Lambda^* = \min_{\eta}\ & \gamma \\
\text{s.t.}\quad & \gamma \geq \mathcal{W}_{\boldsymbol{\xi}}\ \forall \boldsymbol{\xi} \in \mathcal{I} \\
& \boldsymbol{\lambda_\xi} \geq 0\ \forall \boldsymbol{\xi} \in \mathcal{I} \\
& C'\boldsymbol{\lambda_\xi} = \boldsymbol{f}\ \forall \boldsymbol{\xi} \in \mathcal{I} \\
& 0 \leq \boldsymbol{\Psi_\xi} \leq Y_{F,\mathbf{s^T}}(\boldsymbol{\Psi_\xi})V\ \forall \boldsymbol{\xi} \in \mathcal{I} \\
& \boldsymbol{\Psi_\xi} \leq (1 - Y_{F,\mathbf{s^T}}(\boldsymbol{\Psi_\xi}))V + Y_{F,\boldsymbol{\lambda_\xi}}(\boldsymbol{\Psi_\xi})\ \forall \boldsymbol{\xi} \in \mathcal{I} \\
& \boldsymbol{\Psi_\xi} \geq (Y_{F,\mathbf{s^T}}(\boldsymbol{\Psi_\xi}) - 1)V + Y_{F,\boldsymbol{\lambda_\xi}}(\boldsymbol{\Psi_\xi})\ \forall \boldsymbol{\xi} \in \mathcal{I} \\
& A \in \mathcal{A}
\end{aligned} \tag{11}$$

where $\mathcal{W}_{\boldsymbol{\xi}} = \mathcal{J}(Z,\mathbf{s}^T,\boldsymbol{\lambda_\xi},\{\boldsymbol{\Psi_\xi}\},F)$ for $Z(\mathbf{s}^T,\boldsymbol{\lambda_\xi}) \triangleq \mathbf{c}'_{\boldsymbol{\xi}}\boldsymbol{\lambda_\xi}$, $\boldsymbol{\Psi_\xi} \in \mathbb{R}^{|(\mathcal{G}(Z,\mathbf{s}^T,\boldsymbol{\lambda_\xi})|}$, $\eta = \{\gamma, A\} \cup (\cup_{\boldsymbol{\xi}\in\mathcal{I}}(\{\boldsymbol{\lambda_\xi}\} \cup \{\boldsymbol{\Psi}_\xi\}))$, F is a bijective map (as defined in Definition 3) from $\mathcal{G}(Z,\mathbf{s}^T,\boldsymbol{\lambda_\xi})$ to $\{\boldsymbol{\Psi}_\xi\}$, and $V = \max(1, \sum_{i\in\mathcal{B}} b_i^o \mathbb{1}_{\mathbb{R}_+}(b_i^o))$.

Now that we have turned Problem (6) into a large-scale single-level MILP, it can be solved to global optimality using column and constraint generation ([26] and [27]). Please see E-Companion VIII for details on how we can tailor the column-and-constraint-generation procedure to the global optimization of Problem (6). Please also see E-Companion XI for a proof that this procedure converges in finite steps to a globally optimal solution of Problem (6).

V. Maximum Efficacy of Reactance Tweaking in Reducing the Post-Disturbance Load Shed

So far, we have focused on the worst-case scenario for measuring the efficacy of reactance tweaking. However, this measure of efficacy might not be sufficient as disturbances are most often not the worst-case. There could be non-extreme scenarios where reactance tweaking is quite effective. It is thus necessary to also capture the efficacy of this post-disturbance control mechanism in the face of the full array of $N-k$ scenarios, not just the worst case. To that end, below we introduce a general notion of efficacy that we can then use to establish an upper bound (i.e. a best-case scenario) on the capability of reactance tweaking in dealing with any $N-k$ disturbance.

Definition 4: The *efficacy* ($E(\kappa)$) of post-disturbance reactance tweaking in response to a given disturbance κ is defined as the total savings in the amount of load shed purely as the contribution of this mechanism. In other words, if $R(\kappa)$ denotes the load satisfied after disturbance κ while using reactance tweaking as a control mechanism, and $Q(\kappa)$ denotes the load that could be satisfied without using this mechanism for the same disturbance, then $E(\kappa) = R(\kappa) - Q(\kappa)$.

Definition 5: The *constant-reactance post-contingency control* problem is the yield maximization problem in which the SO has no control over line reactances, and can be formulated as the following LP:

$$\begin{aligned}
\max_{d}\ & \sum_{i\in\mathcal{B}} b_i^d \\
\text{s.t.}\quad & I_{ijh}^{T+1} x_{ijh}^o + \Upsilon(s_{ijh}^T - 1) \leq (\theta_i^{T+1} - \theta_j^{T+1}), \\
& \forall (i,j,h) \in \mathcal{E} \\
& I_{ijh}^{T+1} x_{ijh}^o + \Upsilon(1 - s_{ijh}^T) \geq (\theta_i^{T+1} - \theta_j^{T+1}), \\
& \forall (i,j,h) \in \mathcal{E} \\
& b_i^g - b_i^d = \sum_{(i,j,h)\in\mathcal{E}_i} I_{ijh}^{T+1}, \quad \forall i \in \mathcal{B} \\
& -\overline{C}_{ijh}^a s_{ijh}^T \leq I_{ijh}^{T+1} \leq \overline{C}_{ijh}^a s_{ijh}^T,\ \forall (i,j,h) \in \mathcal{E} \\
& 0 \leq b_i^g \leq \overline{b}_i^g, \quad \forall i \in \mathcal{B} \\
& 0 \leq b_i^d \leq \overline{b}_i^d, \quad \forall i \in \mathcal{B} \\
& \theta_i^{T+1}, I_{ijh}^{T+1}, b_i^g, b_i^d \in \mathbb{R}, \forall i \in \mathcal{B}, (i,j,h) \in \mathcal{E}
\end{aligned} \tag{12}$$

where $d = \{\boldsymbol{\theta}^{T+1}, \mathbf{I}^{T+1}, \mathbf{b}^g, \mathbf{b}^d\}$. We shall write this LP in standard form as

$$\max_{W\boldsymbol{\varpi}\leq\boldsymbol{\nu}} \boldsymbol{p}'\boldsymbol{\varpi} \tag{13}$$

We can now derive a tight upper bound (best-case scenario) on the efficacy of post-disturbance reactance tweaking among the set of all possible $N-k$ disturbances for a given k and a given bus load scenario, as shown in the theorem below.

Theorem 4: For a given k, let us denote the set of all "$N-k$" disturbances by $\mathcal{K}(k)$. For a given vector of bus injections $\mathbf{b}^o$, the efficacy of post-disturbance reactance tweaking in response to any $\kappa \in \mathcal{K}(k)$ is upper bounded as follows:

$$\begin{aligned}
E(\kappa) \leq\ & \max_{\Pi} \sum_{i\in\mathcal{B}} b_i^d - \mathcal{J}(\mathcal{U},\mathbf{s}^T,\boldsymbol{\pi},\{\boldsymbol{\Theta}\},F) \\
\text{s.t.}\quad & \boldsymbol{\pi} \geq 0 \\
& W'\boldsymbol{\pi} = \boldsymbol{p} \\
& 0 \leq \boldsymbol{\Theta} \leq Y_{F,\mathbf{s}^T}(\mathbf{s}^T)V \\
& \boldsymbol{\Theta} \leq (1 - Y_{F,\mathbf{s}^T}(\boldsymbol{\Theta}))V + Y_{F,\boldsymbol{\pi}}(\boldsymbol{\Theta}) \\
& \boldsymbol{\Theta} \geq (Y_{F,\mathbf{s}^T}(\boldsymbol{\Theta}) - 1)V + Y_{F,\boldsymbol{\pi}}(\boldsymbol{\Theta}) \\
& \omega \in \Omega;\ \ a \in \tilde{a}
\end{aligned}$$

TABLE I
WORST-CASE-SCENARIO EFFICACY

k	$E(\kappa^*)$	% Load Satisfied by SO's Control
2	0	93.19%
3	0	89.16%

TABLE II
BEST-CASE EFFICACY

T	Maximum Savings in Load Shed
0	42.0 MW
1	60.7 MW

and this upper bound is tight. Here, $\Pi = \{A, \omega, \boldsymbol{\pi}, \boldsymbol{\Theta}\}$, $\mathcal{U}(\mathbf{s}^T, \boldsymbol{\pi}) \triangleq \boldsymbol{\nu}'\boldsymbol{\pi}$, F is a bijective map (as defined in Definition 3) from $\mathcal{G}(\mathcal{U}, \mathbf{s}^T, \boldsymbol{\pi})$ to $\{\boldsymbol{\Theta}\}$, $\boldsymbol{\Theta} \in \mathbb{R}^{|(\mathcal{G}(\mathcal{U}, \mathbf{s}^T, \boldsymbol{\pi})|}$, and $V = \max(1, \sum_{i \in \mathcal{B}} b_i^o \mathbb{1}_{\mathbb{R}_+}(b_i^o))$.

VI. NUMERICAL EXPERIMENTS

In this section, we shall present the results of our numerical experiments on the IEEE One-Area RTS-1996 test case system [28], which has 24 buses (11 generators and 16 buses with load) and 38 lines (please see E-Companion XII for a diagram of this system). The numerical experiments were performed in MATLAB, and Gurobi [29] was used for solving the MILPs. The operating range of the reactance tweaking devices were set within the range reported for TCSC in [5]; according to [5], for the capacitive characteristic of TCSC (i.e. for decreasing line reactance) the maximum value is fixed at -0.8 times the line reactance, and for the inductance (i.e. for increasing line reactance) the maximum is 0.2 times the line reactance.

In our numerical experiments below, we will present results for cases with $k = 2$ and $k = 3$; nevertheless, our methodology works for $k = 4$ or any higher-order k, as the MILP framework provided in the above results holds for any value of k.

A. Efficacy in the Event of a Worst-Case Disturbance

In the first set of numerical experiments, we focus on the worst-case efficacy of reactance tweaking in the RTS-1996 test system. In these experiments, we set $k \in \{2, 3\}$, $H = 3$ (i.e. we allow tweaking the reactances of up to only three lines), and $T = 0$. We use a base load flow scenario adopted from the dataset for the IEEE One-Area RTS-1996 test case system [28]. At this load level, prior to the disturbance the system is serving 2850 MW of load in total. Table I displays the results for this set of experiments (note that in this table, κ^* denotes the worst-case disturbance obtained from solving Problem 6).

The results in Table I suggest that reactance tweaking on up to 3 transmission lines cannot increase the worst-case resilience of the RTS-1996 system to a disturbance caused by removing 2 or 3 lines.

B. Best-Case Efficacy

To give a more comprehensive perspective into the efficacy of reactance tweaking, we next focus on its "best-case scenario" as defined in the previous section. In these experiments, we first set $k = 3$ and $H = 2$. In the first step, using the same base load flow scenario as above, we set $T = 1$ and compute (using the MILP derived in Theorem 4) that the total amount of savings in load-shedding as a pure contribution of reactance tweaking (i.e. $E(\kappa)$) is tightly upper bounded by 60.7 MW for this case. That is about 2.13% of the total demand. Then, we set $T = 0$ for the same load level and the tight upper bound on $E(\kappa)$ drops to 42 MW. This is summarized in Table II.

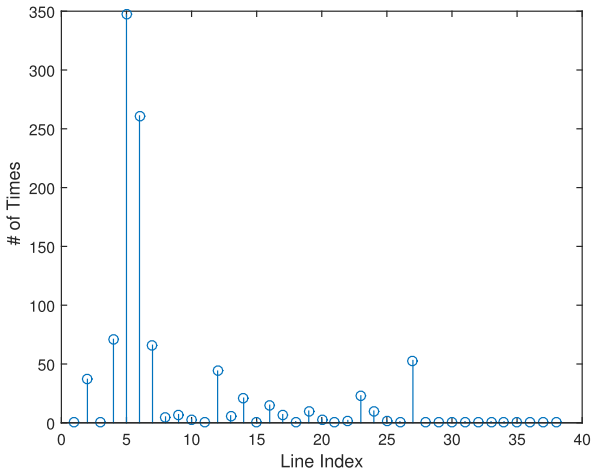

Fig. 1. Number of samples in which each line was chosen as one of the two optimal lines to tweak (for $k = 3$).

Next, we randomize the load at each demand bus such that it is sampled from a uniform distribution over the support $[L_i^N - 0.1L_i^N, L_i^N + 0.1L_i^N]$ where L_i^N is the base load at bus i. So, we are allowing for up to 10% uncertainty in the load at each demand bus relative to the base load. We set $T = 0$ and run this experiment 500 times for 500 different realizations of the random vector of bus loads. We observe that the value of the upper bound on $E(\kappa)$ among these 500 trials ranges from 34.3 MW to 71.8 MW with mean 45.9 MW and standard deviation 6.8 MW. Fig. 1 shows the number of times (out of 500 randomly sampled load levels) that each line was chosen post-contingency as one of the two optimal lines to tweak the reactance of.

An immediate observation in Fig. 1 is that several of the lines indexed from 1 through 14 have been chosen more frequently for reactance tweaking than almost all the lines indexed 15 onward. Looking at the locations of lines $1 - 14$, an immediate observation is that almost all the lines indexed $1 - 14$ are located in the southern part of the power system (please see Fig. 4 in E-Companion XII), and that part of the system is demand-rich as shown in the diagram (i.e. most of the demand buses in the system are located in the southern part).

We repeat the above experiment for $H = 3$ and $H = 1$, while keeping all other parameters the same as above. Increasing the number of tweaking devices (H) from 2 to 3 **does not** change the average bound on savings (i.e. average among 500 samples), and the same two lines (i.e. lines 5 and 6) are the modes. The line triplet that maximally benefits from tweaking is $\{5, 6, 12\}$. As can be seen in the system diagram in Fig. 4 and the table of line indexes (in E-Companion XII), line 5 connects bus 2 to 6, line 6 connects bus 3 to 9, and line 12 connects bus 8 to bus 9.

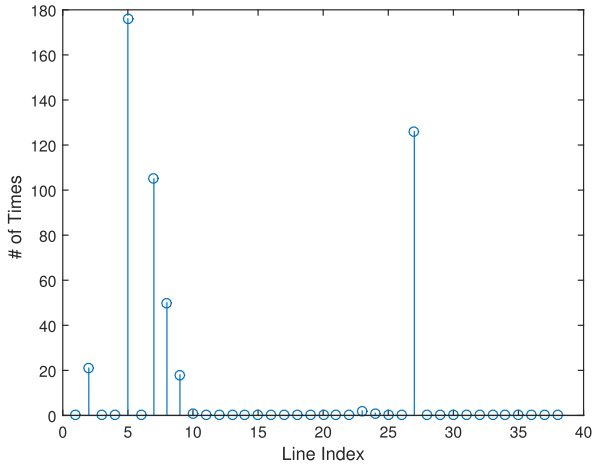

Fig. 2. Number of samples in which each line was chosen as the only optimal line to tweak (for $k = 3$).

Decreasing the number of tweaking devices (H) from 2 to 1 decreases the average upper bound on savings among 500 samples to 33.9 MW (i.e. the average bound on savings decreases by 12 MW compared to the case of $H = 2$ which had an average savings of 45.9 MW as reported earlier in this section).

Fig. 2 shows the number of times that each line was chosen post-contingency as the single optimal line to tweak. Note in Fig. 2 that for $H = 1$, line 5 (connecting bus 2 to 6) is still the mode. Recall that for $H = 2$, line 5 was the mode but line 6 also had been selected as an optimal line to tweak in a large number of trials. But this time line 6 is never the optimal line for reactance tweaking in the 500 trials, and instead lines 7 (connecting bus 3 and 24) and 27 (connecting bus 15 and 24) have each appeared over 100 times as the optimal line to tweak the reactance of.

This observation is compelling and could have non-trivial implications for optimal placement of reactance tweaking devices in this transmission system, especially when it comes to deciding how many such devices are useful for the system. However, the problem of optimal placement of reactance-tweaking devices is not a topic of interest in this study and merits its own line of research, and we leave a deeper investigation of these observations to future research.

Remark 5: The newly-added constraints in the column-and-constraint-generation algorithm are expected to be strong [26], and according to [1] the algorithm usually converges after a small number of iterations. However, it is possible for the algorithm to take many iterations to converge, and to the best of our knowledge, the limit of its scalability has not been established and remains a future research direction. Also, the run time of these bilevel optimization algorithms can generally be boosted by "warm-start" initial feasible solutions. Thus, exploring heuristics for finding high-quality initial feasible solutions is also another important avenue for future research. One can then combine those initialization heuristics with cloud computing for solving these bilevel optimization problems on networks of various scales in order to rigorously establish the trade-offs regarding run time as the size of the problem increases, and provide insights into the limits of its scalability.

VII. Conclusion

In this paper we developed optimization formulations for assessing the efficacy of transmission line reactance tweaking as a post-disturbance control mechanism using two different measures of system resilience. We gave a rigorous MILP reformulation scheme to facilitate the global optimization of the bilevel non-convex MINLP corresponding to the worst-case efficacy of this mechanism. We also derived a MILP formulation for computing an exact upper bound (best-case efficacy) on the amount of load saved post-disturbance as a pure contribution of reactance-tweaking in dealing with any $N - k$ contingency for a given k. A main feature of our model is its ability to track the multi-stage evolution of cascading failures before the SO's post-disturbance response.

Although the economic viability, engineering design, and implementation of a post-disturbance reactance-tweaking technology are not discussed in this paper, our results can potentially motivate researchers to dig deeper into this idea and cover various aspects of such technology as interesting future research problems. Naturally, a reactance tweaking device (e.g. TCSC) would have applications way beyond post-disturbance control. Thus, another major future direction could be to develop a comprehensive framework for identifying optimal locations of these devices for post-disturbance control purposes among other applications.

Finally, developing heuristics for initializing the bilevel optimization process with warm starts, and also exploring the use of cloud services for large-scale networks, are other important avenues for future research as far as run time and scalability are concerned.

Acknowledgment

This work was presented in A. Faghih's Ph.D. dissertation titled "On control and optimization of cascading phenomena in a class of dynamic networks," Massachusetts Institute of Technology, Cambridge, MA, USA, 2015.

References

[1] L. Zhao and B. Zeng, "Vulnerability analysis of power grids with line switching," *IEEE Trans. Power Syst.*, vol. 28, no. 3, pp. 2727–2736, Aug. 2013.

[2] P. Trodden, W. Bukhsh, A. Grothey, and K. McKinnon, "Optimization-based islanding of power networks using piecewise linear AC power flow," *IEEE Trans. Power Syst.*, vol. 29, no. 3, pp. 1212–1220, May 2014.

[3] J. Arroyo and F. Fernandez, "A genetic algorithm approach for the analysis of electric grid interdiction with line switching," in *Proc. Int. Conf. Intell. Syst. Appl. Power Syst.*, 2009, pp. 1–6.

[4] Y. Lu and A. Abur, "Static security enhancement via optimal utilization of thyristor-controlled series capacitor," *IEEE Trans. Power Syst.*, vol. 17, no. 2, pp. 324–329, May 2002.

[5] S. Gerbex, R. Cherkaoui, and A. J. Germond, "Optimal location of multi-type FACTS devices in a power system by means of genetic algorithms," *IEEE Trans. Power Syst.*, vol. 16, no. 3, pp. 537–544, Aug. 2001.

[6] J. Paserba, N. Miller, E. Larsen, and R. Piwko, "A thyristor controlled series compensation model for power system stability analysis," *IEEE Trans. Power Del.*, vol. 10, no. 3, pp. 1471–1478, Jul. 1995.

[7] C. Canizares and Z. Faur, "Analysis of SVC and TCSC controllers in voltage collapse," *IEEE Trans. Power Syst.*, vol. 14, no. 1, pp. 158–165, Feb. 1999.

[8] R. Billinton, M. Fotuhi-Firuzabad, and S. Faried, "Power system reliability enhancement using a thyristor-controlled series capacitor," *IEEE Trans. Power Syst.*, vol. 14, no. 1, pp. 369–374, Feb. 1999.
[9] N. Acharya and N. Mithulananthan, "Influence of TCSC on congestion and spot price in electricity market with bilateral contract," *Elect. Power Syst. Res.*, vol. 77, no. 8, pp. 1010–1018, Jun. 2007.
[10] S. Singhand and A. David, "Optimal location of FACTS devices for congestion management," *Elect. Power Syst. Res.*, vol. 58, no. 2, pp. 71–79, Jun. 2001.
[11] P. Tiwari and Y. Sood, "An efficient approach for optimal allocation and parameters determination of TCSC with investment cost recovery under competitive power market," *IEEE Trans. Power Syst.*, vol. 28, no. 3, pp. 2475–2484, Aug. 2013.
[12] D. Bienstock and A. Verma, "The $n - k$ problem in power grids: New models, formulations, and numerical experiments," *SIAM J. Optim.*, vol. 20, no. 5, pp. 2352–2380, Apr. 2010.
[13] J. Arroyo, "Bilevel programming applied to power system vulnerability analysis under multiple contingencies," *IET Gener., Transmiss. Distrib.*, vol. 4, no. 2, pp. 178–190, Feb. 2010.
[14] A. Pinar, J. Meza, V. Donde, and B. Lesieutre, "Optimization strategies for the vulnerability analysis of the electric power grid," *SIAM J. Optim.*, vol. 20, no. 4, pp. 1786–1810, Feb. 2010.
[15] V. Donde, V. Lopez, B. Lesieutre, A. Pinar, C. Yang, and J. Meza, "Severe multiple contingency screening in electric power systems," *IEEE Trans. Power Syst.*, vol. 23, no. 2, pp. 406–417, May 2008.
[16] J. Salmeron, K. Wood, and R. Baldick, "Worst-case interdiction analysis of large-scale electric power grids," *IEEE Trans. Power Syst.*, vol. 24, no. 1, pp. 96–104, Feb. 2009.
[17] V. Bier, E. Gratz, N. Haphuriwat, W. Magua, and K. Wierzbickiby, "Methodology for identifying near-optimal interdiction strategies for a power transmission system," *Rel. Eng. Syst. Saf.*, vol. 92, no. 9, pp. 1155–1161, Sep. 2007.
[18] A. Motto, J. Arroyo, and F. Galiana, "A mixed-integer LP procedure for the analysis of electric grid security under disruptive threat," *IEEE Trans. Power Syst.*, vol. 20, no. 3, pp. 1357–1365, Aug. 2005.
[19] A. Delgadillo, J. Arroyo, and N. Alguacil, "Analysis of electric grid interdiction with line switching," *IEEE Trans. Power Syst.*, vol. 25, no. 2, pp. 633–641, May 2010.
[20] T. Kim, S. Wright, D. Bienstock, and S. Harnett, "Analyzing vulnerability of power systems with continuous optimization formulations," *IEEE Trans. Netw. Sci. Eng.*, vol. 3, no. 3, pp. 132–146, Jul. 2016.
[21] Q. Ba and K. Savla, "Robustness of DC networks with controllable link weights," *IEEE Trans. Control Netw. Syst.*, vol. 5, no. 3, pp. 1479–1491, Sep. 2018.
[22] B. Geißler, A. Martin, A. Morsi, and L. Schewe, "Using piecewise linear functions for solving MINLPs," in *Mixed Integer Nonlinear Programming* (The IMA Volumes in Mathematics and Its Applications), vol. 154, J. Lee and S. Leyffer, Eds. New York, NY, USA: Springer, 2012, pp. 287–314.
[23] A. Bergen and V. Vittal, *Power Systems Analysis*, 2nd ed. Upper Saddle River, NJ, USA: Prentice-Hall, 2000.
[24] A. Molina-Garcia, F. Bouffard, and D. Kirschen, "Decentralized demand-side contribution to primary frequency control," *IEEE Trans. Power Syst.*, vol. 26, no. 1, pp. 411–419, Feb. 2011.
[25] G. Glanzmann and G. Andersson, "Coordinated control of FACTS devices based on optimal power flow," in *Proc. 37th Annu. North Amer. Power Symp.*, 2005, pp. 141–148.
[26] B. Zeng and L. Zhao, "Solving two-stage robust optimization problems using a column-and-constraint generation method," *Oper. Res. Lett.*, vol. 41, no. 5, pp. 457–461, Sep. 2013.
[27] L. Zhao and B. Zeng, "An exact algorithm for two-stage robust optimization with mixed integer recourse problems," Dept. Ind. Manage. Syst. Eng., Univ. South Florida, Tampa, FL, USA, 2012. [Online]. Available: https://pdfs.semanticscholar.org/6b15/8459656b321a0791cc9df4a09af161c8f5e2.pdf
[28] C. Grigg *et al.*, "The IEEE reliability test system–1996. A report prepared by the Reliability Test System Task Force of the Application of Probability Methods Subcommittee," *IEEE Trans. Power Syst.*, vol. 14, no. 3, pp. 1010–1020, Aug. 1999.
[29] Gurobi Optimization Inc., Houston, TX, USA. *Gurobi Optimizer Reference Manual Version 6.0.2.*, 2015.